European Journal of Pharmaceutics and Biopharmaceutics 94 (2015) 393–403

Contents lists available at ScienceDirect

European Journal of Pharmaceutics and Biopharmaceutics

journal homepage: www.elsevier.com/locate/ejpb

Research Paper

The *in vivo* fate of nanoparticles and nanoparticle-loaded microcapsules after oral administration in mice: Evaluation of their potential for colon-specific delivery

Yiming Ma [a,b], Adrian V. Fuchs [a,b], Nathan R.B. Boase [a,b], Barbara E. Rolfe [a], Allan G.A. Coombes [c], Kristofer J. Thurecht [a,b,d,*]

[a] Australian Institute of Bioengineering and Nanotechnology, The University of Queensland, Brisbane, Australia
[b] Centre for Advanced Imaging, The University of Queensland, Brisbane, Australia
[c] The International Medical University, School of Pharmacy, No. 126 Jalan Jalil Perkasa 19, Bukit Jalil, 57000 Kuala Lumpur, Malaysia
[d] ARC Centre of Excellence in Convergent BioNano Science and Technology, Australia

ARTICLE INFO

Article history:
Received 19 March 2015
Revised 11 June 2015
Accepted in revised form 12 June 2015
Available online 25 June 2015

Keywords:
Colorectal cancer
Oral delivery
Nanoparticles
Chitosan–hypromellose microcapsules
In vivo
Animal optical imaging

ABSTRACT

Anti-cancer drug loaded-nanoparticles (NPs) or encapsulation of NPs in colon-targeted delivery systems shows potential for increasing the local drug concentration in the colon leading to improved treatment of colorectal cancer. To investigate the potential of the NP-based strategies for colon-specific delivery, two formulations, free Eudragit® NPs and enteric-coated NP-loaded chitosan–hypromellose microcapsules (MCs) were fluorescently-labelled and their tissue distribution in mice after oral administration was monitored by multispectral small animal imaging. The free NPs showed a shorter transit time throughout the mouse digestive tract than the MCs, with extensive excretion of NPs in faeces at 5 h. Conversely, the MCs showed complete NP release in the lower region of the mouse small intestine at 8 h post-administration. Overall, the encapsulation of NPs in MCs resulted in a higher colonic NP intensity from 8 h to 24 h post-administration compared to the free NPs, due to a NP 'guarding' effect of MCs during their transit along mouse gastrointestinal tract which decreased NP excretion in faeces. These imaging data revealed that this widely-utilised colon-targeting MC formulation lacked site-precision for releasing its NP load in the colon, but the increased residence time of the NPs in the lower gastrointestinal tract suggests that it is still useful for localised release of chemotherapeutics, compared to NP administration alone. In addition, both formulations resided in the stomach of mice at considerable concentrations over 24 h. Thus, adhesion of NP- or MC-based oral delivery systems to gastric mucosa may be problematic for colon-specific delivery of the cargo to the colon and should be carefully investigated for a full evaluation of particulate delivery systems.

1. Introduction

Current chemotherapy for colorectal cancer usually involves continuous intravenous infusion of potent anti-cancer drugs such as 5-fluorouracil via an in-dwelling catheter that has unsatisfactory efficacy and severe side effects [1,2]. Oral formulations delivering chemotherapeutics to the colon are promising to improve treatment of colorectal cancer [3], driven by the principle that targeted delivery of drugs to their intended cellular targets offers opportunities for increasing treatment efficacy while minimising the administered dose and associated side effects. Novel drug delivery systems based on nanotechnology, such as nanoparticles (NPs) [4] and nanoparticle-in-microcapsule systems [5], have recently been developed for achieving colon-specific delivery of therapeutic agents. Studies have shown that drug-loaded NPs can exhibit higher anti-cancer activity than the corresponding drug alone by enhancing the solubility of poorly water soluble drugs and increasing drug uptake by cancer cells [6,7]. Moreover, conjugation of targeting ligands to NPs could increase delivery of drugs to tumour cells through greater specificity, thus minimising the effect on surrounding tissue [8,9]. Encapsulation of NPs in microcapsules has also been demonstrated to avoid premature degradation or uptake of NPs during their passage through the upper gastrointestinal tract, thus increasing the delivery of NPs to the colon for enhanced therapeutic efficacy [10,11].

* Corresponding author at: Room 408, Building 57, Centre for Advanced Imaging, The University of Queensland, Brisbane, QLD 4072, Australia. Tel.: +61 7 33460344.
E-mail address: k.thurecht@uq.edu.au (K.J. Thurecht).

http://dx.doi.org/10.1016/j.ejpb.2015.06.014
0939-6411/

To gain a full understanding of the effectiveness of NPs or nanoparticle-in-microcapsule systems for colorectal cancer chemotherapy, it is necessary to elucidate the *in vivo* fate of NPs and/or microcapsules following oral administration, especially the distribution and retention of the particles in the colorectal region. For the nanoparticle-in-microcapsule system, the precision of *in vivo* release of NPs from microcapsules would provide significant insight into the evaluation of the system for targeting cancer cells in the colorectal region. However, the reported NP-based delivery vehicles are usually evaluated by tissue distribution studies which look at concentration of encapsulated drugs in collected tissues and/or therapeutic effects [4,5,10,11], and the *in vivo* fate of the formulations has not been well understood.

Thus, the aim of the present study was to investigate the *in vivo* distribution of NPs in mice in real-time following oral administration of the two typically reported NP-based formulations, un-encapsulated NP suspension and NP-loaded microcapsules. The model NPs were encapsulated in a conventional colon-targeting microcapsule carrier to examine whether the microcapsules could release the incorporated NPs specifically in the colon. We believe that such a study would broaden the current understanding on the development of oral delivery systems for treating colorectal cancer, as well as other diseases in the gastrointestinal tract such as inflammatory bowel diseases.

An important experimental design criterion for colorectal delivery systems is that the model NPs must be prepared from a material that (1) prevents premature drug release in the upper gastrointestinal tract, (2) exhibits the required stability in the colon, and (3) promotes drug uptake into tumour cells or local drug release. The Eudragit® series of copolymers are esters of acrylic and methacrylic acid and have pH-dependent solubility as determined by the monomer compositions and their functionalities. Eudragit® RS PO is a cationic, water insoluble polymer that has been exploited to prolong drug release while increasing the cellular uptake of nanoparticles due to its net positive charge [12]. Moreover, the concentration of Eudragit® RS in sustained release dosage forms can be conveniently measured using UV–visible spectrophotometry after forming an ion-pair complex with tropaeolin OOO [13].

The microcapsule system investigated in this study was prepared from chitosan and hypromellose (HPMC) and then coated by Eudragit® S100, which for these materials have been well reported for preparing colon-specific delivery systems [14–17]. Our previous study [18] of alginate carriers for colon delivery of Eudragit® RS PO NPs showed that electrostatic complexation between the positively charged NPs and negatively charged alginate retarded NP release from the alginate carrier. In order to prevent NP-carrier binding and aggregation, chitosan and hypromellose were selected to prepare the microcapsule carrier for this study, based on their positive and neutral charge, respectively. Eudragit® S100 dissolves above pH 7 and provides a stable and insoluble shell in the low pH environment encountered in the stomach and upper regions of the small intestine. It becomes soluble under the higher pH conditions encountered in the lower regions of the small intestine and colon, subsequently facilitating release of the NPs in this region.

In order to investigate the tissue distribution of Eudragit® RS NPs after oral administration of both formulations, determination of the concentrations of the NPs in each section of the animal gastrointestinal tract is necessary. Optical fluorescence imaging provides a high signal-to-noise ratio *in vivo* and has been explored as a direct and non-invasive tool for tracking NPs in live animals, and providing qualitative and quantitative analysis of tissue distribution [19–23]. In this study, Eudragit® RS PO lacks the functionality for attachment of fluorescent dyes; therefore, we synthesised a companion polymer with similar properties (poly(methyl methacrylate), (PMMA)) that was pre-labelled with a fluorescent dye (Cy5) and then blended with Eudragit® RS PO to produce a fluorescent NP model (Cy5 NPs).

As for the NP-in-microcapsule system, it was important to determine the kinetics of the *in vivo* release of the NPs from Eudragit® S100-coated chitosan–HPMC MCs as well as the concentration of NPs released in the colon arising from specificity of the delivery vehicle. Thus, a multi-spectral approach was employed whereby the Cy5 NPs were loaded into MCs which had been pre-labelled with a second fluorophore exhibiting different optical properties. The MC carrier system was labelled with IR750 dye through amidation of chitosan before prior to blending with hypromellose to prepare MCs. This strategy enabled a quantitative analysis of the biodistribution of each component of the carrier system (NPs and MCs) along the full length of the mouse gastrointestinal tract following oral administration to monitor the *in vivo* course of NP release from MCs.

2. Experimental section

2.1. Materials

Eudragit® RS PO and Eudragit® S100 were provided by Evonik Industries (Darmstadt, Germany). Hypromellose E50 (HPMC) was provided by Colorcon Asia Pacific Pty. Ltd. Medium molecular weight chitosan (75–85% deacetylated, molecular weight 190,000–310,000 Da) and sodium phosphate tribasic dodecahydrate were purchased from Sigma Aldrich. Cyanine 5 amine (Cy5-NH_2) was purchased from Lumiprobe Corporation, USA and IRDye® 750 NHS Ester from LI-COR Biosciences, USA. Phosphate buffered saline (PBS) tablets were purchased from Amresco Inc. (Solon, OH). Tropaeolin OOO (pH 11.0–13.0) was purchased from British Drug Houses Ltd. Dimethyl sulfoxide (DMSO) and ethyl acetate of analytical grade were purchased from Chem-supply (SA, Australia). Pentafluorophenol was purchased from Matrix Scientific (South Carolina, USA). Methacrylic acid and methyl methacrylate (Sigma Aldrich) were passed through basic alumina before use to remove inhibitor. All other chemicals were purchased from Sigma Aldrich and used as received. Mouse embryonic fibroblast cells (NIH/3T3; ATCC® CRL-1658™) and human colon adenocarcinoma cells (HT-29; ATCC® HTB-38™) were cultured in Dulbecco's modified Eagle medium (DMEM) (Lonza, Australia) and RPMI Medium 1640 (Gibco) respectively containing 10% foetal bovine serum (Moregate BioTech, Australia), penicillin/streptomycin and glutamine (Gibco) in an atmosphere of 5% CO_2 in air.

2.2. Synthesis and characterisation of Cy5-labelled poly(methyl methacrylate) polymer (PMMA)

PMMA was synthesised bearing fluorescent groups as a surrogate drug molecule and incorporated into the nanoparticle formulation for tracking in the digestion tract. Full synthetic procedures are presented in Supporting Information.

2.3. Preparation and characterisation of Cy5-labelled PMMA-Eudragit® RS PO nanoparticles (Cy5 NPs) (Scheme 1-1)

Cy5 NPs were prepared from a mixture of Cy5-labelled PMMA and Eudragit® RS PO using a modified emulsification-diffusion method reported by Nguyen et al. [24]. Cy5-labelled PMMA (25 mg) and Eudragit® RS PO (225 mg) were dissolved in 5 mL *n*-butanol and the solution was added to distilled water (20 mL) using a 30G needle at a rate of 1.5 mL/min (Harvard Apparatus PHD 2000 Syringe Pump) under magnetic stirring at 1500 rpm. The resulting emulsion was stirred for 4 days at room temperature to evaporate the *n*-butanol completely and then centrifuged at

4000 rpm for 5 min to remove any polymer precipitate. The supernatant was collected and the NP yield was obtained by freeze drying aliquots of the Cy5 NP suspension. The labelling efficiency in dried Cy5 NPs was determined by fluorescence spectrophotometry (Horiba Fluoromax-4, Ex = 648 nm, Em = 670 nm) following dissolution of a known weight of NPs in DMSO and expressed as the weight ratio of Cy5 dye to NPs. A known set of concentrations of Cy5 dye dissolved in DMSO in the linear range of 0.025–0.25 μg/mL was used to produce the calibration curve.

The Z-average size (Z-ave), polydispersity index (PDI) and zeta potential of Cy5 NPs were determined in triplicate at a final concentration of 1 mg/mL using a Zetasizer Nano ZS (Malvern Instruments, Malvern, UK) at an angle of 173°. To examine the morphology of Cy5 NPs, a drop of NP suspension (100 μg/mL) was placed on a carbon coated copper grid (100 mesh). After 5 min, the excess fluid was blotted with a filter paper and the grid was negatively stained with uranyl acetate (1%, w/v). Excess stain was removed by further blotting. The grid was air-dried and examined by transmission electron microscopy (TEM, Jeol 1010, USA) at 100 kV.

2.4. Preparation and characterisation of Cy5 NP-loaded IR750 chitosan–hypromellose microcapsules coated with Eudragit® S100 (Eudragit® S100-coated Cy5 NP-in-IR750 MCs, Scheme 1-2; Scheme 1-3)

Cy5 NPs were encapsulated in chitosan–hypromellose microcapsules using the conventional ionotropic gelation technique [25]. Nitrogen gas was used to aid the formation of MCs by modifying the laboratory-scale spray equipment reported by Si et al. [26]. Briefly, 1 mL of Cy5 NP suspension (30 mg/mL) was mixed with 0.5 mL of HPMC (40 mg/ml) at 500 rpm and then added to 1.5 mL of IR750 chitosan solution (30 mg/mL – synthetic procedure described in Supporting Information). The suspension was sprayed through a 23G needle into a 1:4 mixture of ethanol in a 5% w/v trisodium phosphate cross-linking solution (65 mL) at a flow rate of 0.15 mL/min. The spray pressure generated by the nitrogen gas was optimised beforehand to provide MC sizes smaller than 300 μm. The resulting suspension of MCs was stirred overnight to ensure complete cross-linking of the MC shell. The Cy5 NP-in-IR750 MCs were collected by centrifugation at 3000 rpm for 4 min and washed twice with distilled water to remove excess trisodium phosphate on the MC surface. The concentration of the MC suspension was determined by freeze drying aliquots of the suspension and weighing lyophilised MCs. Cy5 NP loading of dried IR750 MCs was measured by slightly modifying the Tropaeolin OOO method reported by Melia et al. [13]. Briefly, Tropaeolin OOO forms an ion-pair complex with the quaternary ammonium groups in Eudragit® RS PO. When extracted into an organic phase, the complex gives rise to an absorbance at 487 nm which is linearly related to polymer concentration. Tropaeolin OOO was dissolved in 0.1 M NaCl solution at a concentration of 2.25 mg/mL. A 200 μL aliquot of the Cy5 NP-in-IR750 MC suspension was added to 0.1 M hydrochloric acid (200 μL) in a centrifuge tube and vortexed for 3 min. This resulted in breakdown of the MC structure and thus released the Cy5 NPs. Then chloroform (0.5 mL) was added to extract the Eudragit® RS PO. After an additional 5 min vortex, the sample was centrifuged at 4000 rpm for 10 min and the supernatant was discarded. Tropaeolin OOO in NaCl solution (150 μL) was added and vortexed for 10 min to obtain extraction into the Eudragit solution in chloroform. After centrifugation at 4000 rpm for 10 min, the bottom chloroform layer was dried in a vacuum oven overnight to remove chloroform. The resulting Tropaeolin OOO-Eudragit® RS PO complex was dissolved in 10 μL of DMSO and analysed using a UV–visible spectrophotometer (NanoDrop 2000, Thermo Scientific, Australia) at a wavelength of 487 nm. Absorbance readings were compared with a calibration curve produced using a series of known concentrations of Eudragit® RS PO (12.5–62.5 μg/mL) in 0.1 M hydrochloric acid. Samples were prepared in triplicate and the NP loading of MCs was expressed as a weight percentage of Eudragit® RS PO in the dried MCs.

Coating of Cy5 NP-in-IR750 MCs was carried out using Eudragit® S100 at a weight ratio of 1.5:1 of MCs. 5 mL of MC suspension in distilled water containing 100 mg MCs was added to Eudragit® S100 in methanol solution (5 mL, 3% w/v) under gentle magnetic stirring. After 1 h incubation, distilled water (20 mL) was added to the suspension and the methanol was evaporated overnight. Coated MCs were collected by centrifugation at 3000 rpm for 3 min and finally re-suspended in 4 mL of distilled water.

The size distribution of Cy5 NP-in-IR750 MCs after Eudragit® S100 coating was determined using dynamic light scattering (Malvern Mastersizer 2000, Malvern, UK). The sample size was measured three times at 25 °C. The Cy5 NP distribution in hydrated Eudragit® S100-coated IR750 MCs was examined using confocal microscopy (LSM 710, Carl Zeiss Inc., Germany).

2.5. In vitro Cy5 NP release from Eudragit® S100-coated Cy5 NP-in-IR750 MCs

The *in vitro* NP release experiment was conducted using a procedure described in a previous study [18]. Simulated gastric and intestinal fluids and incubation times were used to mimic the *in vivo* pH environments and transit times that MCs would encounter as they travel along the human gastrointestinal tract [27–31]. Briefly, 1 mL of the Eudragit® S100-coated Cy5 NP-in-IR750 MC suspension was centrifuged at 2500 rpm for 5 min after which the supernatant was removed to avoid its dilution effect on the release medium. Sedimented microcapsules were incubated with 1.5 mL of simulated gastric fluid (SGF, 0.05 M HCl, pH 1.2) for 2 h at 37 °C, then transferred to 1.5 mL simulated intestinal fluid (SIF, pH 6.8, PBS) for 6 h, and finally to 1.5 mL of simulated colonic fluid (SCF, pH 7.4 PBS) for 6 h. Samples were prepared in triplicate and 1 mL of release medium was collected every hour using a pipette tip wrapped with mesh cut from a Falcon™ cell strainer (mesh size: 40 μm) to avoid infiltration of MCs into the collected release samples. Centrifugation was not utilised for release sample collection since multiple centrifuge steps were previously shown to accelerate the disintegration of alginate MCs [18]. Results of NP characterisation showed that Eudragit® RS PO was the major component of Cy5 NPs and quantification of released NPs based on assay of Eudragit® RS PO had a lower limit of quantification than Cy5-based assay (experimental data not shown). Thus, Cy5 NP concentration in the release media was assayed by the Tropaeolin OOO method and compared to calibration standards of Eudragit® RS PO in each release medium. In the collected SIF and SCF release samples, dissolved Eudragit® S100 from the MC coating may bind with positive Eudragit® RS PO and hinder complex formation between tropaeolin dye and Eudragit® RS PO during partition between the aqueous and chloroform phases. Therefore, 400 μL of each release sample was acidified by adding 20 μL of HCl (1 M) and precipitated Eudragit® S100 was removed by centrifugation. The pH was re-adjusted to approximately 7 with NaOH (1 M) before adding chloroform to extract the Eudragit® RS PO NPs. The NP release rate was calculated as the ratio of released Eudragit® RS PO NPs against the initial loading in IR750 MCs and expressed as cumulative release (% w/w) versus time (h). Representative release samples were examined by TEM to check the presence of individual (separated) Cy5 NPs which showed successful staining with uranyl acetate.

2.6. In vitro cellular uptake of Cy5 NPs

Mouse fibroblast NIH/3T3 cells and human colon adenocarcinoma HT29 cells (respectively) were cultured in DMEM and RPMI medium supplemented with 1% penicillin/streptomycin, 4 mM L-Glutamine and 10% foetal bovine serum at 37 °C in a humidified atmosphere of 5% CO_2 in air. For flow cytometric analysis, both cell lines were seeded in 6-well plates at a density of 2×10^5 cells/well in 2 mL of complete medium. NIH/3T3 cells were incubated for 24 h and HT29 cells overnight to allow cell attachment. Cells were washed with PBS and incubated with Cy5 NPs suspended in 1 mL culture medium for 1, 2 or 4 h. Cy5 NP concentrations were 50, 100 and 300 μg/mL and samples were prepared in triplicate. Afterwards, cells were washed with PBS to remove unbound Cy5 NPs, trypsinised and then fixed in 1% paraformaldehyde for 15 min prior to analysis using flow cytometry (BD Accuri™ C6, BD Biosciences, Australia). The Student's unpaired t test was used to compare the uptake of Cy5 NPs between the two cell types at each incubation condition. All p values resulted from the use of two-sided tests and $p < 0.05$ was considered significantly different.

For confocal microscopy examination, cells were seeded on coverslips in a 24-well plate at a density of 5×10^4 cells/well in 0.5 mL of culture medium and incubated for 16 h (HT29 cells) or 24 h (NIH/3T3 cells) to allow attachment. Cy5 NP suspension (1 mL, 1.5 mg/mL) was added to each plate. After 4 h incubation, cells were washed with PBS and fixed with 4% paraformaldehyde and nuclei were stained with Hoechst 33342 before observation under a confocal microscope (Zeiss 710 Confocal LSM).

2.7. In vivo biodistribution of Cy5 NPs and Eudragit® S100-coated Cy5 NP-in-IR750 MCs Cy5 NP examined by small animal optical imaging

A total of 20 BALB/c female mice (17–22 g, eight weeks) were used in this study. Animal ethics clearance was approved by the University of Queensland ethical committee (AEC Approval Number: AIBN/288/13/ARC). All animals were fed with a suspension of DietGel®Boost (Clear H_2O®) overnight prior to administration of the MCs to avoid any possible food fibre effects on gastric emptying. The abdomen of each animal was carefully shaved to improve acquisition of the fluorescence signals emitted by Cy5 NPs and the IR750 MC carriers during their transit through the mouse gastrointestinal tract.

The Cy5 NP group was dosed with a suspension of NPs in distilled water (0.3 mL, 1.5 mg Cy5 NPs) via oral gavage. Prior to imaging, animals were anaesthetised (3% isoflurane in oxygen, 1.5 L/min) and placed in an imaging cradle. To elucidate the transit timeline of un-encapsulated Cy5 NPs in mice, five mice were imaged at 0.5, 2, 5, 8 and 24 h after oral administration, with 1 mouse being euthanased at each time point for further *ex vivo* analysis. It was shown that at 0.5 and 2 h post-administration, NPs were mostly located within the stomach and the small intestine. Therefore, no more animals were culled at 0.5 or 2 h for the further *ex vivo* analysis in order to save the animal number to be used. Two additional mice were euthanased at each of 5, 8 and 24 h, respectively ($n = 3$) to improve fluorescence quantitation at these timepoints. For all animals, the gastrointestinal tracts and major organs (liver, kidney, lung, heart, spleen) were removed and imaged. Images were acquired using a Carestream MS FX PRO (Bruker/CareStream, Rochester, NY) in conjunction with Carestream Imaging Software MI. Fluorescence images were collected with excitation/emission at 620 ± 10/700 ± 17.5 nm (Cy5 NP signal), 4 × 4 binning, f-stop 2.80, FOV 190 mm and 60 s acquisition time. X-ray images were also recorded using the following instrument settings: f-stop 2.80, X-ray filter 0.2 mm, FOV 190 mm and 10 s acquisition time. All images were batch exported as 16-bit TIFF images and image processing was completed using Image-J (National Institutes of Health). Fluorescence images were false coloured and overlaid onto X-ray images.

The remaining 9 mice were used for the MC group and dosed via oral gavage with Eudragit® S100 coated Cy5 NP-in-IR750 MCs suspended in distilled water (0.3 mL, equivalent to 0.75 mg Cy5 NPs). 3 animals were imaged at 0.5, 2, 5, 8 and 24 h after oral administration and then euthanased. To gain further insight into the pattern of biodistribution of MCs, two additional sub-groups of 3 animals each were euthanased at 5 and 8 h, respectively ($n = 3$). The gastrointestinal tracts and major organs of all animals were removed following euthanasia and imaged immediately. Fluorescence images were collected with excitation/emission at 620 ± 10/700 ± 17.5 nm (Cy5 NP signal) and 720 ± 10/790 ± 17.5 nm (IR750-labelled chitosan signal), 4 × 4 binning, f-stop 2.80, FOV 190 mm and 60 s acquisition time. X-ray images were also recorded and all images were processed as described above.

The NP doses administered in the both groups were different due to experimental considerations as described below. Our trial experiment showed that un-encapsulated Cy5 NPs were widely distributed and thus diluted within the mouse gastrointestinal tract, leading to problems in detection and measurement of Cy5 intensity due to animal auto-fluorescence. In order to achieve an acceptable signal/noise ratio in the fluorescence images of the NP group, a higher NP dose was administered (double the concentration compared to the MC group). For the MC group, it was difficult to increase the amount of encapsulated Cy5 NPs to the same as the free Cy5 NPs because of the loading of Cy5 NPs in MCs and the suggested maximum oral dosage volume for mice (20 mL/kg body weight [32]). To address this dose-imaging sensitivity issue in future studies, NPs should be prepared with a higher Cy5 labelling efficiency and MCs with an improved NP loading to produce desirable imaging sensitivity. Nonetheless, using these dosing strategies we were able to effectively track the NPs and MC carrier following oral administration.

3. Results and discussion

This study aimed to compare the site-specificity of free NPs and NP-in-MC systems for the colorectal region via the oral route. For the NP-in-MC system, production of a multi-labelled system allowed us to unambiguously ascertain whether the MCs were able to protect their cargo (in this case Cy5 NPs) during passage through the upper gastrointestinal tract, with subsequent release in the colon. Formulation of the multispectral system is described in Scheme 1.

3.1. Characterisation of Cy5-labelled PMMA and IR750-labelled chitosan

In order to effectively quantify the biodistribution and corresponding concentration of NPs and MCs in the mouse gastrointestinal tract, precise analysis of NP and MC labelling efficiency is essential. The molar mass of the Cy5-labelled PMMA was determined using ^{1}H NMR and UV–visible spectrophotometry. The former analysis was performed by comparing the proton signals in the NMR spectrum resulting from the CTA end-groups to the proton signals originating from PMMA repeat units (Mn = 18 kDa). Similarly, the molar mass was calculated using UV–visible spectrophotometry of the CTA end-groups (molar absorptivity: 13,200 M^{-1} cm^{-1} in acetonitrile) to give a M_n of 17.8 kDa. The molar ratio of Cy5 dye to PMMA polymer was determined by both fluorescence and UV–visible spectrophotometry (molar absorptivity: 177,200 M^{-1} cm^{-1}). It was determined that the PMMA contained approximately one Cy5 dye molecule per 20 polymer chains

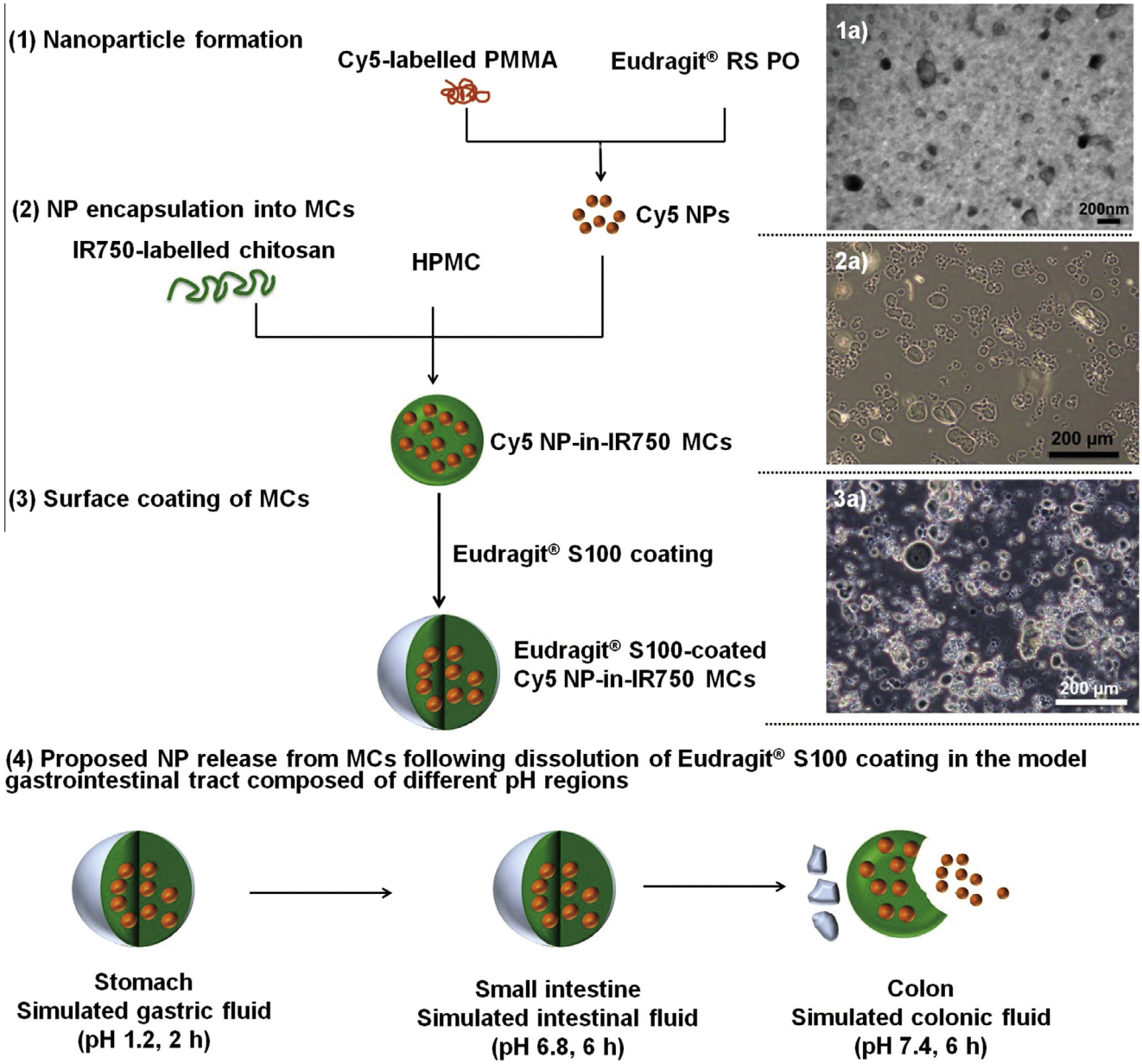

Scheme 1. Design and preparation of the NP-in-MC systems that can be tracked by multispectral optical imaging. For each step, microscopy is used to show morphology of the components within the system. (1a) TEM image of nanoparticles (scale bar 200 nm); (2a) optical micrograph of microcapsules with no coating (scale bar 200 µm); (3a) optical micrograph of microcapsules after coating with Eudragit S100 (scale bar 200 µm). (4) Schematic of the digestive tract showing the various pH regions and residence times that must be considered in the design of carrier systems.

(1.67 ± 0.28 µg of Cy5 dye per mg of PMMA measured by fluorescence spectrophotometry). The IR750-labelled chitosan had a conjugation loading of approximately 2.97 ± 0.15 µg of IR750 dye per mg of chitosan as measured by fluorescence spectroscopy.

3.2. Preparation of Cy5 NPs and Eudragit® S100-coated Cy5 NP-in-IR750 MCs

Cy5 NPs were used in our study as model NPs and a major challenge in NP preparation was the need to obtain a high NP yield with sufficiently high fluorescence intensity to allow detection and quantitative analysis along the gastrointestinal tract of test animals. Thus, unlabelled Eudragit® RS PO was used alone in preliminary studies to optimise NP formulation before incorporation of Cy5-labelled PMMA. Most published nanoprecipitation or emulsion methods [33–35] for Eudragit® RS PO NP preparation involve polymer dissolution in solvents such as acetone and dichloromethane and use of surfactants to stabilise the polymer-organic solution droplets in the aqueous phase to prevent NP aggregation after solvent evaporation. However, application of this conventional approach typically produced a low yield of Eudragit® RS NPs (3–12%, w/w, unpublished data) due to the difficulty in recovering NPs from the viscous, surfactant-containing aqueous phase by ultracentrifugation. In the present study we overcame this issue by using *n*-butanol as the organic phase. Owing to the low interfacial tension between *n*-butanol and water, NPs could be prepared without using surfactants [24].

Eudragit® RS PO NPs were recovered with a high yield of around 70% (w/w) simply by evaporating *n*-butanol completely and subsequently removing polymer flakes by low speed centrifugation. Cy5-labelled NPs prepared in the same way using the mixture of Cy5-labelled PMMA and Eudragit® RS PO had a satisfactory yield

of around 76% (w/w). Laser light scattering revealed a Z-ave diameter of 198.7 nm, a PDI of 0.201 and a Zeta potential of 50.0 ± 6.24 mV for Cy5-labelled NPs. The TEM image (Scheme 1) reveals a NP size range of 30–200 nm without significant aggregation. The weight ratio of Cy5 dye to total polymer in the final dried NPs was (0.0043 ± 0.0005)%.

The Cy5 NPs were loaded into IR750-labelled chitosan–HPMC MCs using spray-aided ionotropic gelation. Ethanol was added to the Na_3PO_4 cross-linking solution (20% v/v) to enhance the formation of spherical MCs and decrease inter-particle interaction [25]. The loading of Cy5 NPs in the lyophilised IR750 MCs was calculated by UV–Vis and found to be fairly high, 10.5 ± 0.4% (w/w) with an encapsulation efficiency of 17.4 ± 0.7%. The yield of IR750 MCs was 58 ± 1.0% (w/w). The spray technique was found to be the main factor leading to the relatively low yield of microcapsules and NP encapsulation efficiency, whereby the high spray pressures employed decreased the efficiency of mixing between the droplets of Cy5 NPs-HPMC-chitosan suspension and the cross-linking solution. NP encapsulation is expected to be improved by modifying process parameters such as the type of chitosan used, solvent, cross-linking solution, and spray pressure.

Optical microscopy (Scheme 1) revealed that the majority of the uncoated Cy5 NP-in-IR750 MCs were less than 100 μm in size while dynamic light scattering measurements revealed that 70% of the particles were within the size range of 50–410 μm in diameter with a (surface weighted) mean diameter of around 100 μm, respectively. The MC diameter slightly increased following coating with Eudragit® S100: 70% of the particles were in the range of 50–430 μm with a surface weighted mean diameter of around 110 μm. Some agglomerates and irregular shaped MCs were evident under the microscope (Scheme 1) which explains the broad particle size range measured by laser light scattering. Confocal microscopy (Fig. 1) revealed an even distribution of Cy5 fluorescence throughout the MCs following coating with Eudragit® S100, suggesting successful incorporation of the model NPs into the MCs. We concluded that the size of the coated Cy5 NP-in-IR 750 MCs obtained here would be suitable for oral gavage in mice. The mouse pylorus diameter was estimated to be 250 μm [36], and a recent report by Jang et al. [37] showed that PMMA MCs (80–300 μm in diameter) were emptied from the stomach of male ICR mice with most of the particles reaching the intestine in less than 4 h.

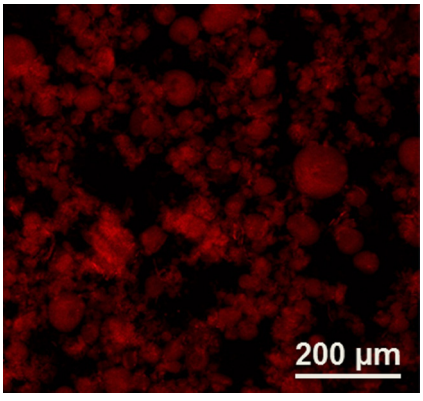

Fig. 1. Confocal microscopic image of the Eudragit® S100-coated Cy5 NP-in-IR750 MCs. Cy5 NP signal is shown in red. The fluorescence of the IR750-MCs could not be observed because its excitation wavelength (760 nm) is out of the wavelength range of the lasers used for confocal acquisition, but homogeneous distribution of the NPs throughout the MC carrier is evident. (For interpretation of the references to colour in this figure legend, the reader is referred to the web version of this article.)

3.3. In vitro Cy5 NP release from Eudragit® S100-coated IR750 MCs

The *in vitro* release behaviour of Cy5 NPs from Eudragit® S100-coated IR750 MCs is shown in Fig. 2. The cumulative NP release was typically confined to less than 4% during 2 h incubation in simulated gastric fluid and subsequent 6 h in simulated intestinal fluid. Over the following 6 h in simulated colonic fluid, a further 9% of the Cy5 NP load was released from the MCs, corresponding to a total cumulative release of approximately 13%. The low release rate may result from slow dissolution of the Eudragit® S100 coating in simulated colonic fluid (pH 7.4) and this impeded NP diffusion through the chitosan–HPMC matrix network. TEM analysis of simulated colonic release medium at 4 h revealed discrete spherical regions on the size scale expected for nanoparticles (50–200 nm) suggesting that the released NPs existed predominantly in an individual (non-aggregated) state (Supporting Information, Fig. S1), while the MC polymeric material is likely the large, diffuse stained regions of soluble polymer in the image. In our study, dynamic laser light scattering could not provide reliable data for the examination of aggregation status of nanoparticles in release samples. The presence of dissolved Eudragit® S100 and chitosan in release samples gave peaks in micro-size range, making data interpretation difficult. Nonetheless, TEM provided a useful method of nanoparticle analysis following release from microcapsules, simulating the release conditions in the colon. The *in vitro* release study predicted that the chitosan–HPMC MC carriers would release approximately 9% of NPs in the colon corresponding to early transit times, indicating that the total release of NPs would take much longer time. Watts et al. [38] reported a mean residence time of 11.0 ± 4.0 h in the human ascending colon for 0.2 mm ion-exchange Amberlite® IR120 resin particles following oral administration and around 80% of dosed particles resided in the colon after 24 h post-administration. Thus the MCs described here are potentially suitable for *in vivo* delivery of non-aggregated NPs to the colon for uptake by cancer cells or local delivery of anti-cancer drugs.

3.4. Cellular uptake of Cy5 NPs by colon cancer HT29 cells and fibroblast NIH/3T3 cells

Following successful demonstration that Cy5 NPs could be released from chitosan–HPMC microcapsules in SCF, it was necessary to confirm their uptake by human colon adenocarcinoma (HT29) cells. We also tested mouse embryonic fibroblast (NIH/3T3) cells in a comparative experiment since these are widely used for *in vitro* cytotoxicity evaluation of biomaterials and NPs [39–41]. Flow cytometric analysis showed that Cy5 NP uptake by HT29 cells and NIH/3T3 cells increased with NP concentration

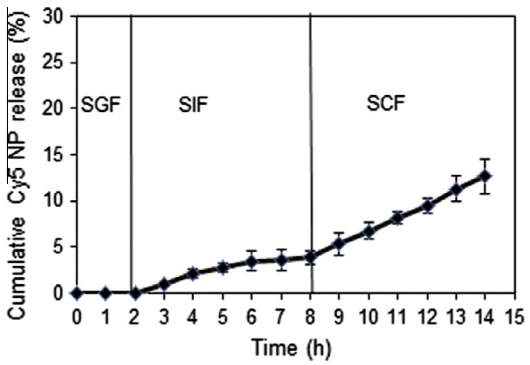

Fig. 2. Cumulative Cy5 NP release from Eudragit® S100-coated IR750 MCs in simulated gastric fluid (SGF), intestinal fluid (SIF) and colonic fluid (SCF) (mean ± SD, $n = 3$).

and incubation time (Fig. 3a). HT29 cells exhibited slightly higher uptake of Cy5 NPs than NIH/3T3 cells under all incubation conditions examined and significant difference between these two cell types was shown when the Cy5 NP concentration or incubation time (alone or both) was used at sufficiently high levels (Cy5 NP concentration 50 μg/mL for 4 h, 100 μg/mL for 2 or 4 h, and 300 μg/mL for all three incubation times) (Fig. 3a). This behaviour was attributed to the higher proliferation rate of cancerous HT29 cells compared with normal NIH/3T3 cells observed during cell culture. The uptake of Cy5 NPs in both cell lines was confirmed by confocal microscopy (Fig. 3b). The high cellular uptake of the NPs shown in the present study may be attributed not only to their small size, but also to their hydrophobicity. Cellular uptake of hydrophobic, polymeric NPs has been widely reported [42,43]. Our *in vitro* data add to the existing body of knowledge that confirms the efficient yet non-specific uptake of NPs by cancerous and normal cells. Conjugating targeting ligands (folate, hyaluronic acid, humanised A33 monoclonal antibody) to NPs has been widely reported in the literature to enhance NP uptake by cancer cells and avoid side effects due to uptake by healthy cells [7,44]. The present

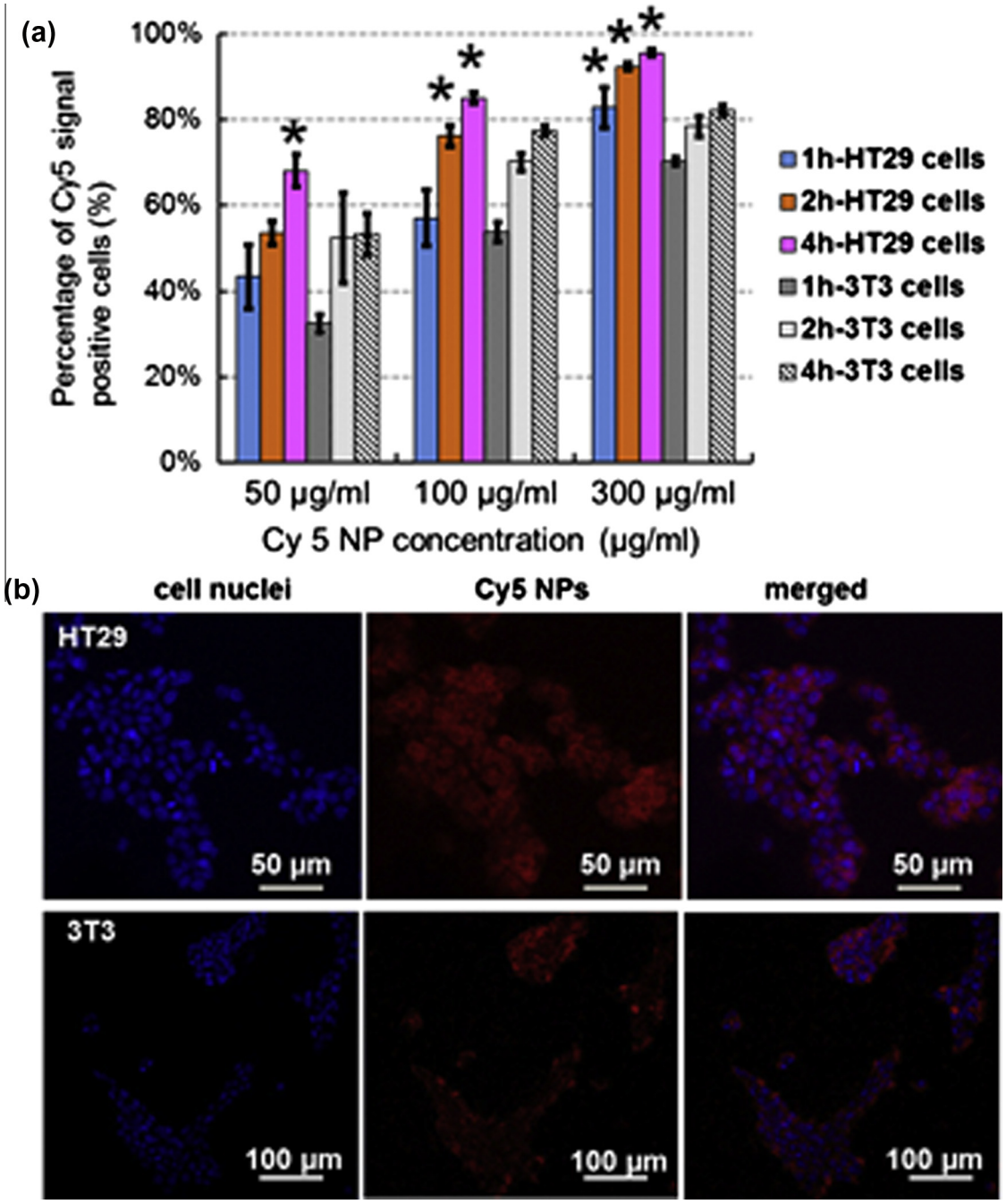

Fig. 3. (a) Flow cytometry analysis of Cy5 NP uptake following incubation with HT29 human colon cancer cells for 1 h (blue), 2 h (orange) or 4 h (pink) and NIH/3T3 mouse fibroblasts for 1 h (black), 2 h (light grey) or 4 h (diagonal lines). Cells were incubated at 50, 100 or 300 μg/mL in complete medium (mean ± SD, $n = 3$/group). Student's unpaired t-test was used to assess statistical difference between the two cell types under each incubation condition (*p value < 0.05). (b) Confocal microscopic images of HT29 (top) and NIH/3T3 cells (bottom) after 4 h incubation with Cy5 NPs (1.5 mg/ml). Left: cell nuclei stained with Hoechst 33342 (blue); middle: Cy5 NP signal (red); right: merged images showing nuclei and Cy5 NPs. (For interpretation of the references to colour in this figure legend, the reader is referred to the web version of this article.)

study of tissue distribution of NPs and the NP-in-MC system paves the way for *in vivo* trials of these promising nanotechnologies for improved treatment and diagnosis of colorectal cancer.

3.5. Biodistribution of free Cy5 NPs and Eudragit® S100-coated Cy5 NP-in-IR750 MCs following oral administration in mice

The biodistribution of Cy5 NPs and the carrier MCs along the mouse gastrointestinal tract following oral administration was analysed using multispectral optical imaging to investigate the specificity of NP delivery to the colon. The progression of Cy5 NP-in-IR750 MCs along the mouse gastrointestinal tract was recorded by whole-body imaging over 24 h (Fig. 4A and B). At 0.5 h, the fluorescence signal arising from both MCs and NPs was predominantly in the stomach and both signals were detected in the abdominal region over 24 h. Owing to the coiling of the large and small intestine within the abdominal cavity, it was difficult to distinguish between the different sections of the gastrointestinal tract. Hence, in order to accurately assess particle biodistribution, the mouse gastrointestinal tracts and major organs were removed at different time points and imaged for quantitative *ex vivo* analysis (Fig. 4C and D). It was found that the IR750 MC carriers were cleared more rapidly from the mouse gastrointestinal tract compared to the released Cy5 NPs, probably due to the MC size and hydrophilicity of the chitosan polymer which would be exposed after dissolution of the Eudragit® S100 coating in the intestinal environment. This observation is significant since it confirms release of NPs from the MC carrier *in vivo*. The other major organs (liver, kidney, lung, heart, spleen) gave rise only to very weak fluorescence signals at all timepoints, typically equivalent to the levels of autofluorescence detected in control mice (Supporting Information, Fig. S2). This indicates that there is minimal absorption of NPs, MCs or 'free' dye molecules into the bloodstream. In contrast, Lee et al. [22] reported some accumulation of Cy5.5-conjugated ZnO nanoparticles around 20 nm and 100 nm in rat kidneys and liver at 7 h following oral administration, illustrating the importance of NP material and size factors in determining the *in vivo* fate of NPs designed for oral drug delivery.

The relative fluorescence intensity ratio of Cy5 NPs to IR750 MCs was used as an indicator of NP residence or accumulation in different regions of the mouse gastrointestinal tract. For example, a higher Cy5-to-IR750 ratio indicates NP release from the MCs and possibly interaction with mouse intestinal mucosa, resulting in longer retention in gastrointestinal tract than if NPs remained encapsulated by the MC carrier. The initial Cy5 NP-in-IR750 MCs were imaged in an Eppendorf tube prior to oral administration and the relative intensity of Cy5:IR750 was used as the zero time point control where all NPs were encapsulated within the MCs (1.86 ± 0.19, $n = 3$, orange dashed line shown in Fig. 5).

The ratio of the two different fluorophores in each section of the mouse gastrointestinal tract and faecal pellets was measured at 5, 8 and 24 h. At all time points the stomach showed consistently low fluorescence ratios (1.1–2.3), indicating restricted release of NPs due to the Eudragit® S100-coating, remaining intact at gastric pH and thus preventing MC disintegration and premature release of NPs in the stomach. The average Cy5:IR750 ratios in the stomach, small intestine, caecum, colon and faecal pellets at 5 h were similar to the zero time point control, indicating that a fraction of the MCs transited rapidly through the GI tract but was largely intact and NP release was minimal. At 8 h, however, the small intestine, caecum and colon exhibited marked increases in average fluorescence intensity ratios to around 15, 10 and 8, respectively indicating significant NP release from the MCs occurs in the small intestine and lower gastrointestinal tract between 5 h and 8 h. These findings parallel the *in vitro* release data presented in (Fig. 2). Compared to the stomach and faecal pellets, the Cy5:IR750 ratio in small intestine, caecum and colon had a relatively high standard deviation, highlighting the complex influence and interplay of physicochemical and physiological factors on NP release. Such factors include dissolution of the Eudragit® S100 coating on MCs, release

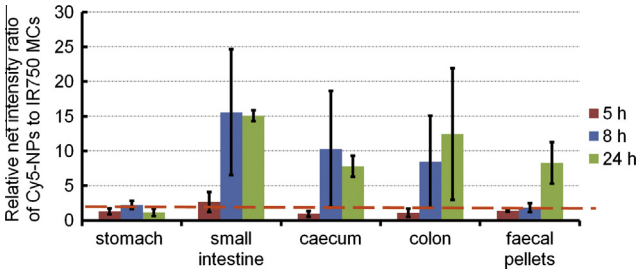

Fig. 5. Fluorescence intensity ratio (Cy5 to IR750) in mouse stomach, small intestine, caecum, colon and faecal pellets at 5, 8 and 24 h after oral administration of Eudragit® S100-coated Cy5 NP-in-IR750 MCs. The dotted orange line shows the relative ratio prior to administration (1.86 ± 0.19 (mean ± SD; $n = 3$)). (For interpretation of the references to colour in this figure legend, the reader is referred to the web version of this article.)

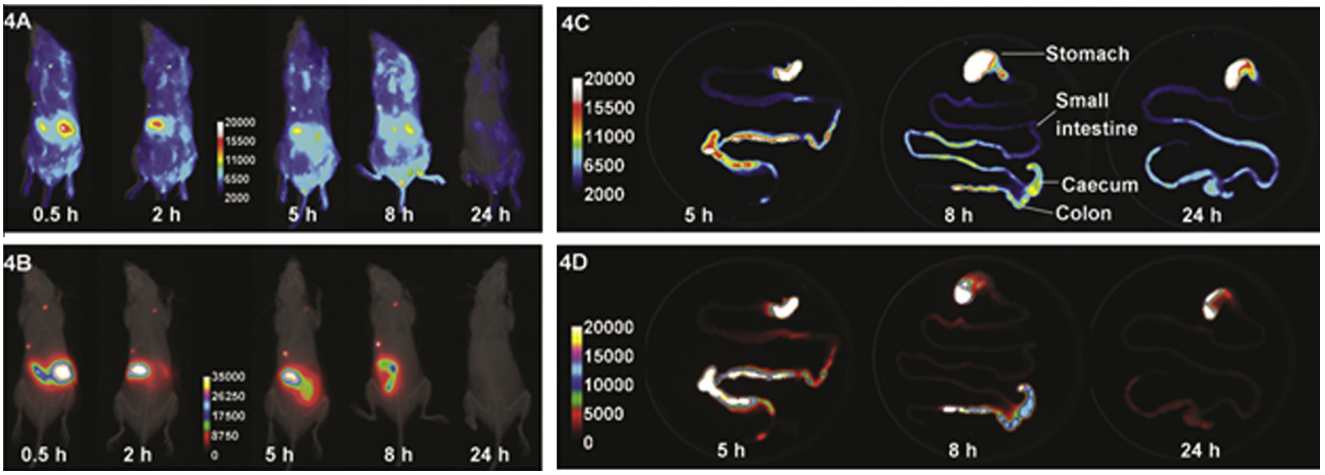

Fig. 4. Mouse whole body images (A and B) at 0.5, 2, 5, 8 and 24 h after oral administration of Eudragit® S100-coated Cy5 NP-in-IR750 MCs. (A) Cy5 NP signal, (B) IR750 MC signal. Fluorescence images of gastrointestinal tract (C and D) following excision from mice at 5, 8 or 24 h after oral administration of Eudragit® S100-coated Cy5 NP-in-IR750 MCs. (C) Cy5 NP signal (D) IR750 MC signal.

of NPs from MCs and the intra-animal variation of transit time within the gastrointestinal tract. Similarly, variation in transit times of poly(epsilon-caprolactone) microspheres (diameter less than 5 μm) through the gastrointestinal tract of Wistar rats has been reported by Bhavsar and Amiji [11]. At 8 h in the present study, the Cy5:IR750 ratio measured in faecal pellets was similar to the zero time-point control and remained much lower than ratios in the small and large intestine, indicating that a fraction of the NP-loaded MCs was excreted intact. At 24 h, however, the intensity ratios in faecal pellets increased to around 8.3 indicating excretion of released NPs. The ratios in the small intestine, caecum and colon at 24 h remained elevated and were similar to the 8 h interval. Taken together, these results showed that the Eudragit® S100-coated IR750 MCs failed to prevent the release of their NP cargo in the small intestine and thus lacked colon-specificity for delivering NPs to the colorectal region. This is despite many reports of carrier systems, similar to the MCs described in this study, exhibiting therapeutic benefits on diseases confined to the colorectal region [45–47]. It is clear from this study that more in-depth studies on the *in vivo* distribution and degradation of these systems are required to gain a better understanding of their colon-targeting ability. It should be noted, however, that release within the lower small intestine as observed for the reported carrier system, still will likely lead to a higher accumulation of drug within the colon compared to the NP system alone.

In order to achieve a greater understanding of the effect of the MC carrier on NP biodistribution, the fluorescence intensity of Cy5 NPs in each section of mouse gastrointestinal tract and faecal pellets after oral administration of encapsulated NPs was compared to that of free Cy5 NPs (Fig. 6). These data are extracted from the *ex vivo* fluorescence images of mouse gastrointestinal tract following oral administration of both formulations at various time points. The distribution profile of free Cy5 NPs within the mouse gastrointestinal tract is shown in Supporting Information, Fig. S3. At 0.5 and 2 h post-administration, the free Cy5 NPs were mostly located within the stomach and the small intestine. At 5 h, their distribution in the lower gastrointestinal tract (caecum, colon) and faecal pellets was noticeably higher than NPs encapsulated by the MCs, reflecting a shorter transit time of un-encapsulated NPs throughout the lower gastrointestinal tract and implying a reduced time period for drug delivery in the colon. NP-loaded MCs showed a stable mean fluorescence intensity of Cy5-labelled NPs in the colon over a 24 h time period and at 24 h was higher than the un-encapsulated NPs. It should be noted that these values are indicative only, since the amount of Cy5 NPs dosed in un-encapsulated NP form was 2 times that of NPs loaded in IR750 MCs (as described in experimental section), suggesting that the NPs would have a limited distribution in the colon if administered in un-encapsulated form. Thus, NP encapsulation in Eudragit® S100-coated chitosan–HPMC MCs avoided rapid transit along gastrointestinal tract and excretion of NPs in faeces, resulting in an increased accumulation of NPs in the colon from 8 h to 24 h post-administration. This behaviour may be expected to facilitate NP interaction with the colorectal wall and localised release of anti-cancer drugs at tumour sites.

Interestingly, both the free Cy5 NPs and Eudragit® S100-coated Cy5 NP-in-IR750 MCs showed significant retention in the stomach over 24 h. Gastric emptying of NPs in rodents typically occurs within 6 h post-administration [48,49]. In the present study, the prolonged retention of the free NPs and NP-in-MCs in the mouse stomach may be attributed to their adhesion to the gastric mucosal surface, which is a continuously secreted protective coating containing proteins, carbohydrates, lipids, salts, antibodies, bacteria, and cellular debris [50]. Particle interaction with gastric mucosa is known to occur via electrostatic, hydrophobic, and van der Waals interactions, polymer chain interpenetration or a combination of these mechanisms [51]. The gastric mucosal surface of many mammals has been shown to be hydrophobic due to its mucin glycoproteins [52] and lipidic constituents, especially the presence of surface-active phospholipids [51]. Additionally, the extensive negatively charged sugar moieties on mucins can bind to positively charged particles through electrostatic interactions [50]. Sakuma et al. [53] reported that polystyrene NPs with cationic polymer chains on the surface exhibited a slower gastric emptying rate in rats compared with their neutral or anionic counterparts. In the present study, the considerable amount of Cy5 NPs in the stomach at 24 h post-administration could be explained by a combination of hydrophobic and electrostatic interaction with gastric mucus (Cy5 NPs are positively charged with a zeta potential of around 50.0 mV). Chickering et al. [54] reported the carboxyl groups of Eudragit® S100 coating on MCs may form hydrogen bonds with mucus glycoproteins, a mechanism that could lead to the observed prolonged retention of the MCs in the stomach.

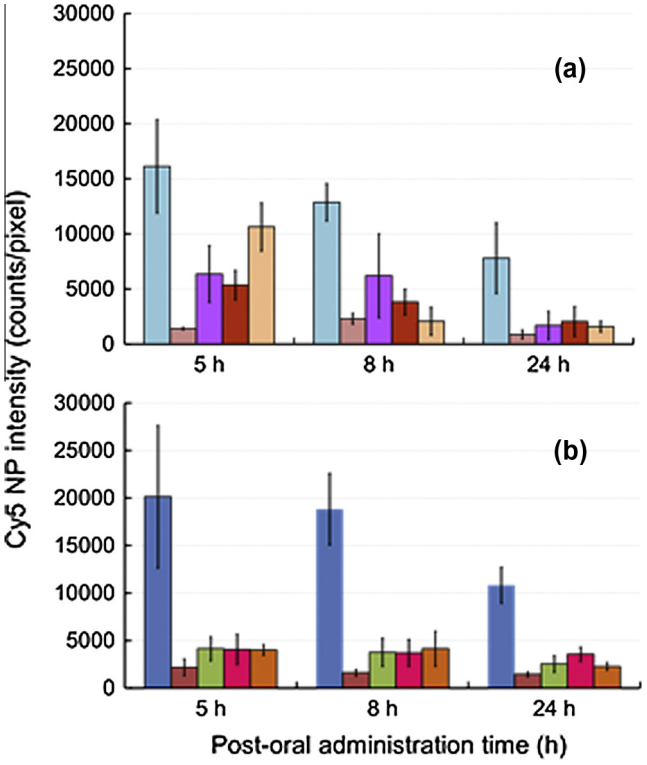

Fig. 6. Fluorescence intensity of Cy5 NPs at 5, 8 and 24 h following oral administration of Cy5 NP suspension (a) and Eudragit® S100-coated Cy5 NP-in-IR750 MCs (b). In each set, data from left to right represent signal arising from stomach, small intestine, caecum, colon and faecal pellets (mean ± SD, n = 3/group). Note that the Cy5 NP dose administered in the form of NP suspension was nearly twice as high as that of the MCs in order to achieve significant signal to noise in the imaging.

It is worthwhile making a final note that the simple *in vitro* release study of colon-targeted drug delivery does not take particle adhesion with stomach mucosa into account (which leads to prolonged particle retention within gastrointestinal tract) and is therefore not the optimum predictor of a delivery system's *in vivo* performance. Also, the *in vitro* model showed a total NP release of only 13% over the time frame investigated while during the *in vivo* study, a complete release of NPs was observed in the lower part of small intestine. These results indicated that the *in vitro* model was not predictive of the *in vivo* NP release from MCs. This was probably because the *in vitro* model did not incorporate all the physiological features of the gastrointestinal tract. Our

study demonstrated that the fluorophore-based animal imaging could be a useful tool for such an *in vivo* evaluation. One experimental concern of this imaging model is that the fluorophore may be widely distributed or metabolised to non-fluorescent moieties following administration, causing difficulty in detection of fluorescent signals in the intended target. Thus, the choice of fluorescent dyes, labelling efficiency of the formulation and dose for administration should be carefully considered when designing the *in vivo* studies, to ensure sufficiently strong fluorescent signals in collected organs of interest for analysis.

4. Conclusions

In the present study, we have compared the tissue distribution of model Eudragit® RS PO NPs in mice following oral administered of the free NP suspension and NP-in-MC formulations. The un-encapsulated NPs exhibited a limited distribution in the colon over 24 h following oral administration. In contrast, the enteric-coated MCs enhanced delivery of NPs to the colon due to prolonged NP residence in the mouse gastrointestinal tract and reduced NP excretion in faeces, although the MCs exhibited poor colon-specificity (i.e. the majority of NP release occurred in the lower small intestine). In addition, this study provided a means to compare *in vitro* and *in vivo* release models. Despite Eudragit® S100-coated chitosan–hypromellose MCs showing restricted release of encapsulated Eudragit® RS PO NPs *in vitro*, a complete NP release from MCs was shown in the lower part of the mouse small intestine following oral administration. Moreover, the results revealed that particle adhesion with stomach mucosa should be investigated during the evaluation of oral delivery systems such as NPs or MCs – this was not predicted by the *in vitro* model. All these results add significantly to our understanding of these colon delivery systems and provide useful design criteria for development of next generation, colon-specific carriers for delivering ligand-conjugated therapeutic or diagnostic NPs to colorectal tumours for improved chemotherapy and detection. The multispectral animal imaging approach utilised for tracking the MC carrier and released NPs in the mouse gastrointestinal tract provided an effective means of evaluating the colon delivery systems and can be equally applied to investigating other oral delivery systems.

Funding sources

Australian Research Council (FT110100284; DP140100951).

ARC Centre of Excellence in Convergent Bio-Nano Science and Technology (CE140100036).

Acknowledgements

The authors would like to thank Mr. Yingdong Zhu (AIBN) for his help with TEM imaging, Ms. Cora Lau for her advice on animal experiments and Prof. Greg Monteith from the School of Pharmacy (UQ) for providing HT29 cells. This work was performed in part at the Queensland node of the Australian National Fabrication Facility, a company established under the National Collaborative Research Infrastructure Strategy to provide nano and micro-fabrication facilities for Australia's researchers. Yiming Ma's PhD studies were supported by the China Scholarship Council and UQ. This work was supported by AIBN, Centre for Advanced Imaging (CAI) at UQ, the Australian Research Council (FT110100284; DP140100951) and was conducted in part within the ARC Centre of Excellence in Convergent Bio-Nano Science and Technology (CE140100036).

Appendix A. Supplementary material

Synthesis and characterisation of Cy5-labelled poly(methyl methacrylate) (PMMA-Cy5) and IRDye® 750-labelled chitosan. TEM images of non-aggregated Cy5 NPs released from MCs after 4 h incubation in simulated colonic fluid. Mouse major organs at 5, 8, 24 h after oral gavage of Eudragit® S100-coated Cy5 NP-IR750 MCs. Mouse gastrointestinal tract and major organs removed at 0.5, 2, 5, 8 and 24 h after oral gavage of Cy5 NP suspension.

Supplementary data associated with this article can be found, in the online version, at http://dx.doi.org/10.1016/j.ejpb.2015.06.014.

References

[1] F.G. Jansman, D.T. Sleijfer, J.C. de Graaf, J.L. Coenen, J.R. Brouwers, Management of chemotherapy-induced adverse effects in the treatment of colorectal cancer, Drug Saf. 24 (2001) 353–367.
[2] H. Kelly, R.M. Goldberg, Systemic therapy for metastatic colorectal cancer: current options, current evidence, J. Clin. Oncol. 23 (2005) 4553–4560.
[3] M.M. Patel, Getting into the colon: approaches to target colorectal cancer, Expert Opin. Drug Deliv. (2014) 1–8.
[4] A. Jain, S.K. Jain, N. Ganesh, J. Barve, A.M. Beg, Design and development of ligand-appended polysaccharidic nanoparticles for the delivery of oxaliplatin in colorectal cancer, Nanomed. – Nanotechnol. Biol. Med. 6 (2010) 179–190.
[5] A.M. Urbanska, E.D. Karagiannis, G. Guajardo, R.S. Langer, D.G. Anderson, Therapeutic effect of orally administered microencapsulated oxaliplatin for colorectal cancer, Biomaterials 33 (2012) 4752–4761.
[6] J. Lu, M. Liong, J.I. Zink, F. Tamanoi, Mesoporous silica nanoparticles as a delivery system for hydrophobic anticancer drugs, Small 3 (2007) 1341–1346.
[7] A. Jain, S.K. Jain, In vitro and cell uptake studies for targeting of ligand anchored nanoparticles for colon tumors, Eur. J. Pharm. Sci. 35 (2008) 404–416.
[8] Y.S. Cho, T.J. Yoon, E.S. Jang, K. Soo Hong, S. Young Lee, O. Ran Kim, C. Park, Y.J. Kim, G.C. Yi, K. Chang, Cetuximab-conjugated magneto-fluorescent silica nanoparticles for in vivo colon cancer targeting and imaging, Cancer Lett. 299 (2010) 63–71.
[9] A.K. Pearce, B.E. Rolfe, P.J. Russell, B.W.C. Tse, A.K. Whittaker, A.V. Fuchs, K.J. Thurecht, Development of a polymer theranostic for prostate cancer, Polym. Chem. 5 (2014) 6932–6942.
[10] A. Lamprecht, H. Yamamoto, H. Takeuchi, Y. Kawashima, A pH-sensitive microsphere system for the colon delivery of tacrolimus containing nanoparticles, J. Control. Release 104 (2005) 337–346.
[11] M.D. Bhavsar, M.M. Amiji, Gastrointestinal distribution and in vivo gene transfection studies with nanoparticles-in-microsphere oral system (NiMOS), J. Control. Release 119 (2007) 339–348.
[12] M. Alai, W.J. Lin, Novel lansoprazole-loaded nanoparticles for the treatment of gastric acid secretion-related ulcers: in vitro and in vivo pharmacokinetic pharmacodynamic evaluation, AAPS J. 16 (2014) 361–372.
[13] C.D. Melia, B.R. Hansraj, K.A. Khan, I.R. Wilding, A simple and rapid method for the quantification of Eudragit RS100 and RL100 poly(methacrylates) in sustained-release dosage forms, Pharm. Res. 8 (1991) 899–902.
[14] M.L. Lorenzo-Lamosa, C. Remunan-Lopez, J.L. Vila-Jato, M.J. Alonso, Design of microencapsulated chitosan microspheres for colonic drug delivery, J. Control. Release 52 (1998) 109–118.
[15] N.K. Thakral, A.R. Ray, D.K. Majumdar, Eudragit S-100 entrapped chitosan microspheres of valdecoxib for colon cancer, J. Mater. Sci. Mater. Med. 21 (2010) 2691–2699.
[16] A. Maroni, M.D. Del Curto, M. Serratoni, L. Zema, A. Foppoli, A. Gazzaniga, M.E. Sangalli, Feasibility, stability and release performance of a time-dependent insulin delivery system intended for oral colon release, Eur. J. Pharm. Biopharm. 72 (2009) 246–251.
[17] E.T. Cole, R.A. Scott, A.L. Connor, I.R. Wilding, H.-U. Petereit, C. Schminke, T. Beckert, D. Cadé, Enteric coated HPMC capsules designed to achieve intestinal targeting, Int. J. Pharm. 231 (2002) 83–95.
[18] Y. Ma, A.G.A. Coombes, Designing colon-specific delivery systems for anticancer drug-loaded nanoparticles: an evaluation of alginate carriers, J. Biomed. Mater. Res. A 102 (2014) 3167–3176.
[19] S. Kunjachan, F. Gremse, B. Theek, P. Koczera, R. Pola, M. Pechar, T. Etrych, K. Ulbrich, G. Storm, F. Kiessling, T. Lammers, Noninvasive optical imaging of nanomedicine biodistribution, ACS Nano 7 (2013) 252–262.
[20] J.H. Na, H. Koo, S. Lee, K.H. Min, K. Park, H. Yoo, S.H. Lee, J.H. Park, I.C. Kwon, S.Y. Jeong, K. Kim, Real-time and non-invasive optical imaging of tumor-targeting glycol chitosan nanoparticles in various tumor models, Biomaterials 32 (2011) 5252–5261.
[21] C.C. Chen, T.H. Tsai, Z.R. Huang, J.Y. Fang, Effects of lipophilic emulsifiers on the oral administration of lovastatin from nanostructured lipid carriers: physicochemical characterization and pharmacokinetics, Eur. J. Pharm. Biopharm. 74 (2010) 474–482.
[22] C.M. Lee, H.J. Jeong, K.N. Yun, D.W. Kim, M.H. Sohn, J.K. Lee, J. Jeong, S.T. Lim, Optical imaging to trace near infrared fluorescent zinc oxide nanoparticles following oral exposure, Int. J. Nanomed. 7 (2012) 3203–3209.

[23] B.E. Rolfe, I. Blakey, O. Squires, H. Peng, N.R.B. Boase, C. Alexander, P.G. Parsons, G.M. Boyle, A.K. Whittaker, K.J. Thurecht, Multimodal polymer nanoparticles with combined 19F magnetic resonance and optical detection for tunable, targeted, multimodal imaging in vivo, J. Am. Chem. Soc. 136 (2014) 2413–2419.
[24] C.A. Nguyen, Y.N. Konan-Kouakou, E. Allemann, E. Doelker, D. Quintanar-Guerrero, H. Fessi, R. Gurny, Preparation of surfactant-free nanoparticles of methacrylic acid copolymers used for film coating, AAPS PharmSciTech 7 (2006) 63.
[25] L. Ma, C. Liu, Preparation of chitosan microspheres by ionotropic gelation under a high voltage electrostatic field for protein delivery, Colloids Surf. B: Biointerfaces 75 (2010) 448–453.
[26] L. Si, Y. Zhao, J. Huang, S. Li, X. Zhai, G. Li, Calcium pectinate gel bead intended for oral protein delivery: preparation improvement and formulation development, Chem. Pharm. Bull. (Tokyo) 57 (2009) 663–667.
[27] H.M. Lai, F. Zhu, W.M. Yuan, N. He, Z.R. Zhang, X.N. Zhang, Q. He, Development of multiple-unit colon-targeted drug delivery system by using alginate: in vitro and in vivo evaluation, Drug Dev. Ind. Pharm. 37 (2011) 1347–1356.
[28] J.M. Hinton, J.E. Lennard-Jones, A.C. Young, A ne method for studying gut transit times using radioopaque markers, Gut 10 (1969) 842–847.
[29] S.S. Davis, J.G. Hardy, J.W. Fara, Transit of pharmaceutical dosage forms through the small intestine, Gut 27 (1986) 886–892.
[30] S.J. Meldrum, H.C. Riddle, G.E. Sladen, B.W. Watson, R.L. Bown, pH profile of gut as measured by radiotelemetry capsule, Br. Med. J. 2 (1972) 104–106.
[31] D.F. Evans, G. Pye, R. Bramley, A.G. Clark, T.J. Dyson, J.D. Hardcastle, Measurement of gastrointestinal pH profiles in normal ambulant human subjects, Gut 29 (1988) 1035–1041.
[32] E.L. McConnell, A.W. Basit, S. Murdan, Measurements of rat and mouse gastrointestinal pH fluid and lymphoid tissue, and implications for in-vivo experiments, J. Pharm. Pharmacol. 60 (2008) 63–70.
[33] K. Dillen, J. Vandervoort, G. Van den Mooter, A. Ludwig, Evaluation of ciprofloxacin-loaded Eudragit® RS100 or RL100/PLGA nanoparticles, Int. J. Pharm. 314 (2006) 72–82.
[34] R. Pignatello, C. Bucolo, P. Ferrara, A. Maltese, A. Puleo, G. Puglisi, Eudragit RS100® nanosuspensions for the ophthalmic controlled delivery of ibuprofen, Eur. J. Pharm. Sci. 16 (2002) 53–61.
[35] N. Ubrich, C. Schmidt, R. Bodmeier, M. Hoffman, P. Maincent, Oral evaluation in rabbits of cyclosporin-loaded Eudragit RS or RL nanoparticles, Int. J. Pharm. 288 (2005) 169–175.
[36] T.T. Kararli, Comparison of the gastrointestinal anatomy, physiology, and biochemistry of humans and commonly used laboratory animals, Biopharm. Drug Dispos. 16 (1995) 351–380.
[37] S.F. Jang, B.A. Goins, W.T. Phillips, C. Santoyo, A. Rice-Ficht, J.T. McConville, Size discrimination in rat and mouse gastric emptying, Biopharm. Drug Dispos. 34 (2013) 107–124.
[38] P.J. Watts, L. Barrow, K.P. Steed, C.G. Wilson, R.C. Spiller, C.D. Melia, M.C. Davies, The transit rate of different-sized model dosage forms through the human colon and the effects of a lactulose-induced catharsis, Int. J. Pharm. 87 (1992) 215–221.
[39] S. Bhatia, A. Yetter, Correlation of visual in vitro cytotoxicity ratings of biomaterials with quantitative in vitro cell viability measurements, Cell Biol. Toxicol. 24 (2008) 315–319.
[40] J. Pan, S.-S. Feng, Targeting and imaging cancer cells by Folate-decorated, quantum dots (QDs)-loaded nanoparticles of biodegradable polymers, Biomaterials 30 (2009) 1176–1183.
[41] K.J. Thurecht, I. Blakey, H. Peng, O. Squires, S. Hsu, C. Alexander, A.K. Whittaker, Functional hyperbranched polymers: toward targeted in vivo 19F magnetic resonance imaging using designed macromolecules, J. Am. Chem. Soc. 132 (2010) 5336–5337.
[42] L. Brannon-Peppas, J.O. Blanchette, Nanoparticle and targeted systems for cancer therapy, Adv. Drug Deliv. Rev. 64 (Suppl.) (2012) 206–212.
[43] K. Yin Win, S.-S. Feng, Effects of particle size and surface coating on cellular uptake of polymeric nanoparticles for oral delivery of anticancer drugs, Biomaterials 26 (2005) 2713–2722.
[44] M.M.J. Kamphuis, A.P.R. Johnston, G.K. Such, H.H. Dam, R.A. Evans, A.M. Scott, E.C. Nice, J.K. Heath, F. Caruso, Targeting of cancer cells using click-functionalized polymer capsules, J. Am. Chem. Soc. 132 (2010) 15881–15883.
[45] T. Bautzova, M. Rabiskova, A. Beduneau, Y. Pellequer, A. Lamprecht, Bioadhesive pellets increase local 5-aminosalicylic acid concentration in experimental colitis, Eur. J. Pharm. Biopharm. 81 (2012) 379–385.
[46] H. Tozaki, T. Odoriba, N. Okada, T. Fujita, A. Terabe, T. Suzuki, S. Okabe, S. Muranishi, A. Yamamoto, Chitosan capsules for colon-specific drug delivery: enhanced localization of 5-aminosalicylic acid in the large intestine accelerates healing of TNBS-induced colitis in rats, J. Control. Release 82 (2002) 51–61.
[47] K. Mladenovska, R.S. Raicki, E.I. Janevik, T. Ristoski, M.J. Pavlova, Z. Kavrakovski, M.G. Dodov, K. Goracinova, Colon-specific delivery of 5-aminosalicylic acid from chitosan–Ca-alginate microparticles, Int. J. Pharm. 342 (2007) 124–136.
[48] K. Yoncheva, L. Guembe, M.A. Campanero, J.M. Irache, Evaluation of bioadhesive potential and intestinal transport of pegylated poly(anhydride) nanoparticles, Int. J. Pharm. 334 (2007) 156–165.
[49] L. Araujo, M. Sheppard, R. Löbenberg, J. Kreuter, Uptake of PMMA nanoparticles from the gastrointestinal tract after oral administration to rats: modification of the body distribution after suspension in surfactant solutions and in oil vehicles, Int. J. Pharm. 176 (1999) 209–224.
[50] L.M. Ensign, R. Cone, J. Hanes, Oral drug delivery with polymeric nanoparticles: the gastrointestinal mucus barriers, Adv. Drug Deliv. Rev. 64 (2012) 557–570.
[51] L.M. Lichtenberger, The hydrophobic barrier properties of gastrointestinal mucus, Annu. Rev. Physiol. 57 (1995) 565–583.
[52] K. Gwozdzinski, A. Slomiany, H. Nishikawa, K. Okazaki, B.L. Slomiany, Gastric mucin hydrophobicity: effects of associated and covalently bound lipids, proteolysis, and reduction, Biochem. Int. 17 (1988) 907–917.
[53] S. Sakuma, R. Sudo, N. Suzuki, H. Kikuchi, M. Akashi, M. Hayashi, Mucoadhesion of polystyrene nanoparticles having surface hydrophilic polymeric chains in the gastrointestinal tract, Int. J. Pharm. 177 (1999) 161–172.
[54] D.E. Chickering Iii, J.S. Jacob, E. Mathiowitz, Bioadhesive microspheres, II. Characterization and evaluation of bioadhesion involving hard, bioerodible polymers and soft tissue, React. Polym. 25 (1995) 189–206.